



The chemistry of iodomethane on MoAl alloy thin films formed on dehydroxylated alumina: Formation and reaction of surface methyl species

Y. Wang, F. Gao, W.T. Tysoe *

Department of Chemistry and Biochemistry, and Laboratory for Surface Studies, University of Wisconsin-Milwaukee, Milwaukee, WI 53211, USA

Received 25 March 2005; accepted for publication 8 June 2005
Available online 13 July 2005

Abstract

The surface chemistry of iodomethane is studied in ultrahigh vacuum using X-ray and Auger spectroscopies and temperature-programmed desorption, on a MoAl alloy film formed by reacting molybdenum hexacarbonyl with dehydroxylated alumina. The alloy is grown by reacting $\text{Mo}(\text{CO})_6$ with a thin alumina film on a molybdenum substrate at 700 K and heating to 1500 K. A portion of the iodomethane dissociates following adsorption at ~ 150 K. Heating to ~ 220 K desorbs molecular iodomethane from the surface leaving adsorbed methyl species and iodine, where the iodine appears to adsorb preferentially on the aluminum. The resulting methyl species can either decompose to deposit carbon and evolve hydrogen, hydrogenate to yield methane or oligomerize yielding predominantly ethylene and propylene, and a small amount of ethane is formed. Both methyl and ethyl radicals are found to desorb from the surface suggesting that the ethylene is formed by methylene insertion into the methyl surface bond to form an ethyl intermediate, which forms ethylene by β -hydride elimination, or hydrogenates to yield ethane. Propylene is likely to form by further methylene insertion into the ethyl-surface bond.

© 2005 Elsevier B.V. All rights reserved.

Keywords: X-ray photoelectron spectroscopy; Temperature-programmed desorption; Auger spectroscopy; Chemisorption; Molybdenum hexacarbonyl; Alumina thin films; Iodomethane; Methyl species

1. Introduction

$\text{Mo}(\text{CO})_6$ has been extensively used to deposit molybdenum on oxides to generate catalysts and/or catalyst precursors [1–12]. Such a procedure has been applied in ultrahigh vacuum to generate

* Corresponding author. Tel.: +1 414 229 5222; fax: +1 414 229 5036.

E-mail address: wtt@uwm.edu (W.T. Tysoe).

model catalysts supported on planer alumina thin films, where surface-sensitive spectroscopic probes can be used to investigate the surfaces and catalytic reactions [13–16]. Our recent studies have shown that reacting $\text{Mo}(\text{CO})_6$ with aluminum [17] and dehydrogenated alumina [18] thin films at 500 K and above forms molybdenum carbide films incorporating a small amount of oxygen. Efforts have been made to perform hydrocarbon conversion reactions on these surfaces and it is found that these surfaces are rather inert. Such inertness has been found recently by Chen et al. [19] by adsorbing O_2 on molybdenum carbide and has been rationalized by site blocking rather than electronic modification effects. Annealing these films to temperatures higher than 1200 K causes CO desorption through alumina reduction by the carbidic carbon, and results in MoAl alloy film formation [17,18].

In the following, the surface chemistry of iodomethane is investigated on the MoAl alloy film. Such a strategy has been extensively used to examine the surface chemistry of hydrocarbons on surfaces since organic iodides tend to decompose by scission of the C–I bonds at relatively low temperatures to deposit hydrocarbon fragments on surfaces, along with chemisorbed iodine [20,21].

It has been shown previously that reaction of low exposures of $\text{Mo}(\text{CO})_6$ with alumina films above 500 K results in the formation of molybdenum carbide nanoparticles on the surface, while higher exposures (of ~ 5000 L of $\text{Mo}(\text{CO})_6$) forms a thin film that completely covers the surface [18]. A MoAl alloy is formed by heating the carbide to ~ 1200 K. The chemistry of hydrogen and CO on MoAl nanoparticles compared with thin films has been investigated to explore particle size effects in these systems [22]. This work explores the chemistry of iodomethane on a MoAl alloy formed by exposing dehydroxylated alumina to 5000 L of $\text{Mo}(\text{CO})_6$ at 700 K and then annealing, to examine the chemistry on the bulk alloy.

Iodomethane is selected for study for a number of reasons. First, the thermal chemistry of methyl species provides insight into understanding many catalytic processes [20,21]. Second, the chemistry on both components of the surface alloy, Mo

and Al, has been investigated previously, where it was found that methyl species start to decompose at ~ 135 K to form methylene species on Mo(100) [23,24]. These persist on the surface to about 200 K and undergo further decomposition at higher temperatures. The only gaseous products are methane and hydrogen, which desorb at ~ 230 and ~ 380 K, respectively. No higher hydrocarbons are detected indicating that C–C bond formation reactions do not occur. The reaction of Al(111) with iodomethane has been investigated by Yates and co-workers [25,26] where $\text{CH}_{3(a)}$, $\text{CH}_{(a)}$ and $\text{I}_{(a)}$, but no $\text{CH}_{2(a)}$ were detected. No gas-phase reaction products were reported. Al–I bond formation was found following CH_3I adsorption on aluminum at 150 K using high-resolution electron energy loss (HREELS), and the depletion of $\text{I}_{(a)}$ from the surface by 650 K was verified by Auger electron spectroscopy (AES).

2. Experimental

Temperature-programmed desorption (TPD) data were collected in an ultrahigh vacuum chamber operating at a base pressure of $\sim 8 \times 10^{-11}$ Torr that has been described in detail elsewhere [13,17,18] where desorbing species were detected using a Dycor quadrupole mass spectrometer placed in line of sight of the sample. This chamber was also equipped with a double-pass, cylindrical-mirror analyzer for collecting Auger spectra.

X-ray photoelectron spectra (XPS) were collected in another chamber operating at a base pressure of $\sim 2 \times 10^{-10}$ Torr, which was equipped with Specs X-ray source and double-pass cylindrical mirror analyzer [17,18]. Spectra were typically collected with a Mg $K\alpha$ X-ray power of 250 W and a pass energy of 50 eV. The deposited film was sufficiently thin that no charging effects were noted and the binding energies were calibrated using the Mo $3d_{5/2}$ feature (at 227.4 eV binding energy) as a standard.

Temperature-programmed desorption spectra were collected at a heating rate of 10 or 15 K/s as indicated. Temperature-dependent XP and Auger spectra were collected by heating the sample to the indicated temperature for 5 s, allowing the

sample to cool to 150 K, following which the spectrum was recorded.

The Mo(100) substrate (1 cm diameter, 0.2 mm thick) was cleaned using a standard procedure, which consisted of argon ion bombardment (2 kV, $1 \mu\text{A}/\text{cm}^2$) and any residual contaminants were removed by briefly heating to 2000 K in vacuo. The resulting Auger spectrum showed no contaminants. Aluminum was deposited onto Mo(100) from a small heated alumina tube, which was enclosed in a stainless-steel shroud to minimize contamination of other parts of the system [27]. The aluminum is oxidized using water vapor at ~ 650 K and subsequently annealed to 1300 K to remove all the hydroxyl groups to form a dehydroxylated alumina thin film [18].

Molybdenum hexacarbonyl (Aldrich, 99%), iodomethane and d_3 -iodomethane (Aldrich, 99.5%) were transferred to glass vials, connected to the gas-handling line of the chamber and purified by repeated freeze-pump-thaw cycles, followed by distillation, and their purities were monitored using mass spectroscopy. These were dosed onto the surface via a capillary doser to minimize background contamination. The exposures in Langmuirs (1 L = 1×10^{-6} Torr s) are corrected using an enhancement factor determined using temperature-programmed desorption (see [13] for a more detailed description of this procedure). H_2 and D_2 (Matheson, >99.5%) were used without further purification.

3. Results

MoAl film formation on dehydroxylated alumina thin film has been described in detail elsewhere [18]. Briefly, it is formed by reacting 5000 L of $\text{Mo}(\text{CO})_6$ with dehydroxylated alumina at 700 K and then annealing to 1500 K. The reaction at 700 K results in MoC_x (where x lies between 0.5 and 1) formation. The resulting carbide film also incorporates a small amount of oxygen. During subsequent annealing, the alumina substrate is reduced by carbidic carbon, resulting in CO formation and desorption, and eventually a MoAl thin film is formed. As shown in Fig. 1, Auger measurement of the freshly formed alloy thin film reveals

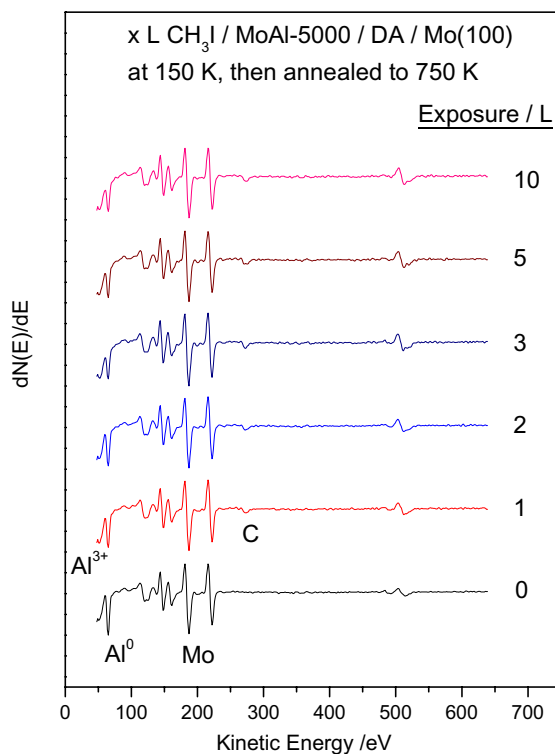


Fig. 1. A series of Auger spectra plotted as a function of iodomethane exposure, where exposures are marked adjacent to the corresponding spectrum collected following iodomethane adsorption on a MoAl alloy film at 150 K and annealing to 750 K. The spectra were collected after allowing the sample to cool to 150 K.

that the alumina features are still detectable (at ~ 53 eV for Al^{3+} and ~ 520 eV for O KLL). Considering that the Auger probe depth is generally ~ 10 Å [28], the thickness of the alloy film should be three to four atomic layers thick, assuming a uniform film. The alloy composition is estimated from the peak-to-peak intensity ratios of the strongest Mo Auger transition (at 186 eV) to that of Al^0 (at 66 eV), corrected for the respective Auger atomic sensitivity factors obtained from [28], to give a Mo/Al ratio of ~ 1.6 . Fig. 1 also displays the Auger spectra of the MoAl alloy film exposed to various amounts of CH_3I at 150 K and subsequently annealed to 750 K. The carbon KLL Auger signal at ~ 270 eV kinetic energy following CH_3I adsorption and annealing, suggests that a portion of the adsorbed CH_3I decomposes. The

low intensity of the carbon signal indicates that decomposition does not occur extensively. However, the weak carbon Auger intensity does not allow the nature of the deposited carbon (whether it is graphitic or carbidic) to be identified. It is found that the intensity of the Al^0 signal at ~ 66 eV decreases with increasing CH_3I exposure. This strongly suggests that some metallic aluminum is oxidized by iodine atoms adsorbed on the surface. The iodine Auger signal appears at approximately the same energy as oxygen (at ~ 520 eV) [28] and the growth in the 520 eV signal with increasing iodomethane exposure indicates that it had dissociated to deposit methyl species and iodine on the surface. In order to explore the dissociation of iodomethane and the subsequent surface chemistry, XP spectra were collected following adsorption of 10 L of CH_3I on the alloy surface, and subsequently annealing to various temperatures, and the results are displayed in Fig. 2 where each spectrum is taken after the sample is cooled to ~ 150 K. Shown in Fig. 2(a) is the Al 2p signal. The initially formed alloy has an Al 2p binding energy of 75.2 eV. This is higher than that of the stoichiometric alumina thin film measured with the same spectrometer (74.6 eV). This shift is induced by an interfacial electrostatic potential caused by electron donation from metallic aluminum [18]. The electron donation from aluminum also results in a molybdenum 3d binding energy lower than that of metallic molybdenum and this effect has been discussed previously [17,18]. Metallic aluminum, since it donates electrons and is finely dispersed, displays a binding energy increase compared to what would be expected for metallic aluminum (~ 72 eV [18]), even though the existence of metallic aluminum is evident from the Auger spectra displayed in Fig. 1. The Al 2p binding energy shifts to 74.8 eV after exposure to 10 L CH_3I at 150 K, a value closer to that of stoichiometric alumina [29]. This suggests, in accord with the Auger results (Fig. 1), that some aluminum is oxidized by iodine. After the sample is annealed to above 1100 K, the Al 2p binding energy returns to 75.2 eV.

Fig. 2(b) displays the corresponding C 1s region. Following CH_3I adsorption at 150 K, a C 1s binding energy of 283.9 eV is found. The signal

intensity decreases at 200 K without apparent chemical shift. The binding energy shifts to 283.3 eV at 250 K and further to 282.7 eV at 300 K and above. Note that all the spectra are collected at 150 K and background CO inevitably adsorbs on the surface at this temperature so that, even after the sample has been heated to 1500 K, a small amount of carbon is still detected. Fig. 2(c) displays the I 3d region where, immediately following adsorption at 150 K, an I $3d_{5/2}$ binding energy is found at 620.0 eV. Molecular iodomethane has an I $3d_{5/2}$ binding energy of 620.3 eV on Pt(111) [30], 620.5 eV on Ni(110) [31] and 620.8 ± 0.1 eV on NiAl surfaces [32] so that the slight shift from these values implies that a portion of the CH_3I has decomposed at 150 K. Complete C–I bond dissociation occurs at 250 K indicated by an I $3d_{5/2}$ binding energy of 619.3 eV, a C 1s binding energy of 283.3 eV [30–32], and the attenuation of the signal indicates that some molecular iodomethane has desorbed. The iodine signal disappears completely on heating to 1200 K. Fig. 2(d) displays the I $3d_{5/2}$ signal area as a function of temperature. Also plotted in Fig. 2(d) as an inset is the corresponding I $3d_{5/2}$ binding energy as a function of temperature. The rapid decrease between 150 and 200 K is assigned to desorption of molecular CH_3I and another sharp decrease between 900 and 1300 K is ascribed to the desorption of iodine from the surface (see below). The much slower decrease between these two regimes is more complicated and this will be discussed in more detail below. An inset to Fig. 2(d) shows that, between 250 and 500 K, the I $3d_{5/2}$ binding energy remains constant at ~ 619.3 eV, but increases to ~ 619.6 eV prior to complete desorption.

The resulting gas-phase products are monitored using temperature-programmed desorption (TPD) collected using a heating rate of 10 K/s in cases where the sample is heated to 750 K, and 15 K/s when the maximum temperature is 1300 K. Fig. 3 displays 71 (CH_3I^{2+}) and 63 amu (I^{2+}) desorption profiles as a function of CH_3I exposure. These m/e ratios are selected since the singly ionized fragments are out of the range (1–100 amu) of the mass spectrometer. At low iodomethane exposures (< 2 L, Fig. 3(a)), no molecular

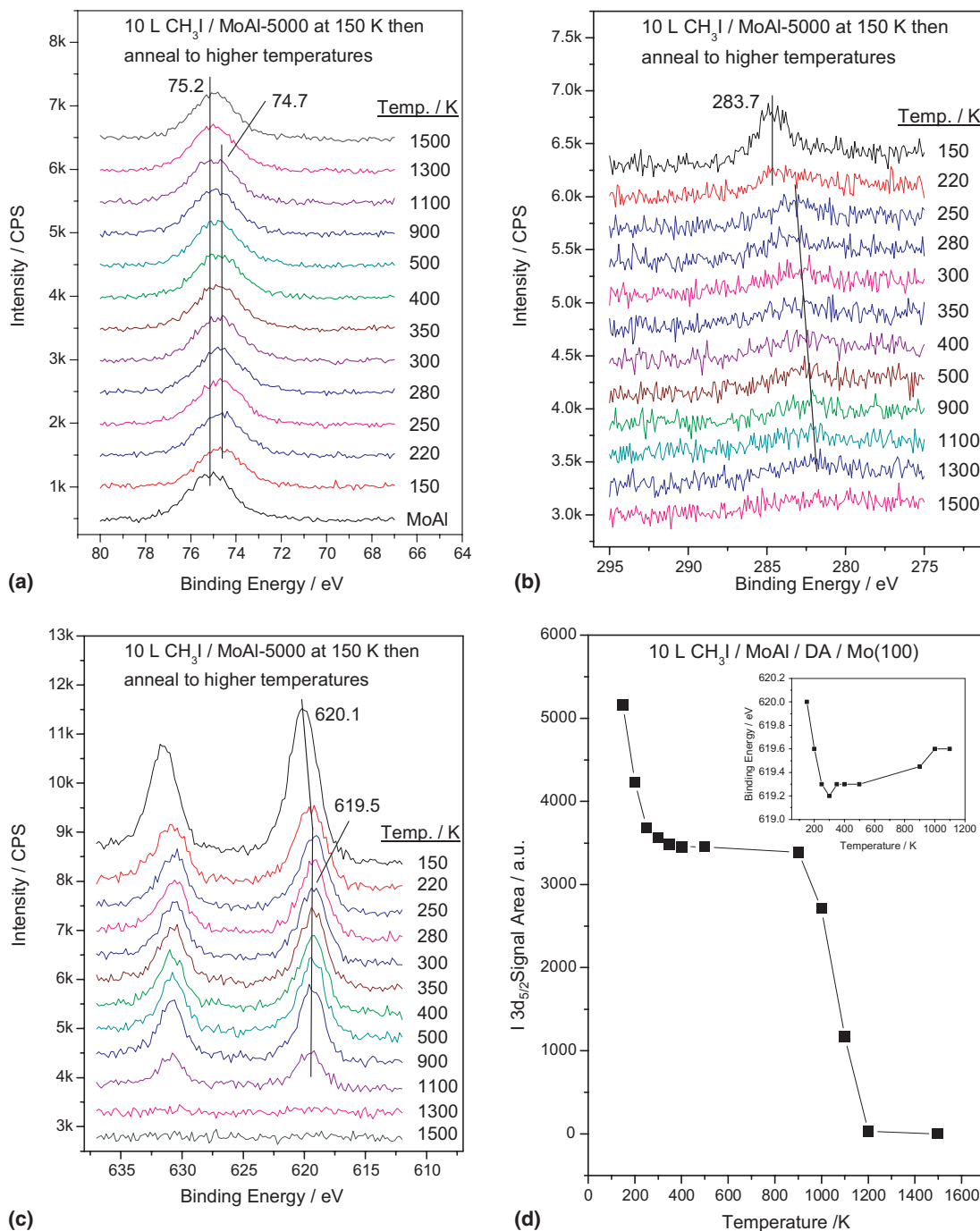


Fig. 2. Narrow scan X-ray photoelectron spectra of (a) Al 2p, (b) C 1s, and (c) I 3d regions collected following the adsorption of 10 L of iodomethane on a MoAl alloy film at 150 K and heating to various temperatures, where annealing temperatures are marked adjacent to the corresponding spectrum. The spectra were collected after allowing the sample to cool to 150 K. Figure (d) plots the integrated area of the I 3d_{5/2} feature (taken from Fig. 2(c)) as a function of annealing temperature. Shown as an inset is the corresponding I 3d_{5/2} binding energy as a function of temperature.

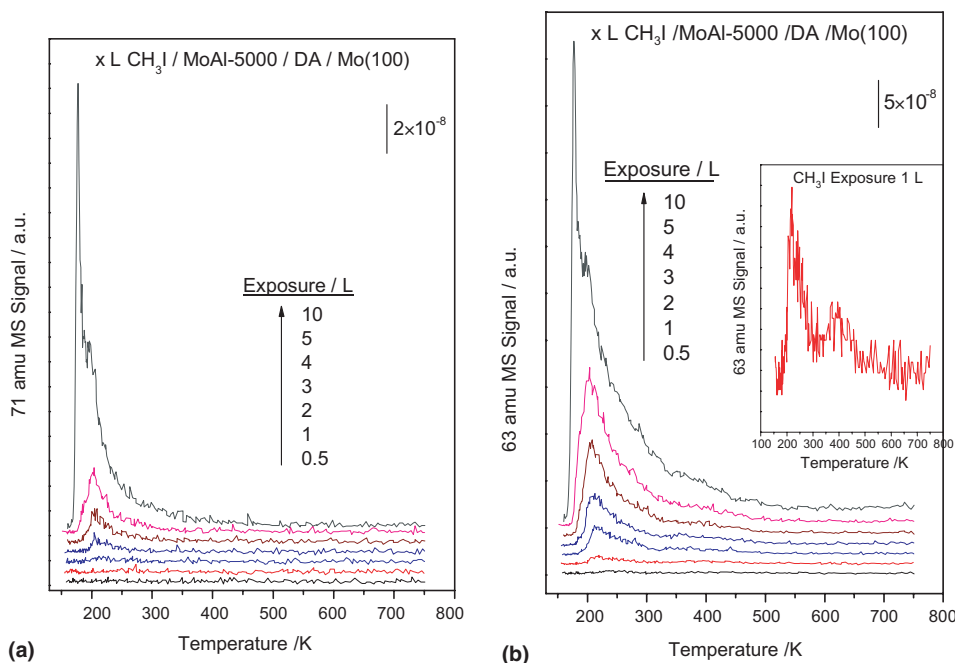


Fig. 3. (a) 71 (CH_3I^{2+}) and (b) 63 amu (I^{2+}) temperature-programmed desorption spectra of iodomethane adsorbed on a MoAl film at 150 K collected using a heating rate of 10 K/s, as a function of CH_3I exposure. Iodomethane exposures are marked adjacent to the corresponding spectrum.

CH_3I desorbs from the surface, suggesting complete cleavage of the C–I bond. At exposures of 2 L and above, a molecular desorption state is centered at 200–210 K in accord with the XPS data plotted in Fig. 2(d). An additional state at ~ 175 K for exposures above 5 L grows indefinitely with exposure and is therefore assigned to CH_3I desorption from second and subsequent layers.

Fig. 3(b) displays the corresponding 63 (I^{2+}) amu profiles. An enlarged TPD trace following a 1 L CH_3I exposure is plotted as an inset. This shows that, while no molecular desorption is found at exposures of 0.5 and 1 L (Fig. 3(a)), iodine desorption is observed in two states: one at ~ 220 K and a less intense one at ~ 400 K. With increasing exposure, the intensities of both states increase, but the low-temperature state intensifies more rapidly. The difference between the 63- and 71-amu profiles suggests that other iodine-containing species may desorb from the surface besides molecular CH_3I .

Fig. 4(a) presents the H_2 desorption profiles. Several desorption states are found, where the

state at ~ 200 K is due to iodomethane fragmentation in the mass spectrometer ionizer and the intensity at ~ 400 K is due to hydrogen adsorption from the background, verified by performing a blank experiment. The state at ~ 370 K, which appears as a shoulder at low iodomethane exposures, is assigned to the thermal decomposition of adsorbed methyl species.

Fig. 4(b) and (c) display the 15 (CH_3) and 16 (CH_4) amu signals respectively. The 15 amu signal is a fragment of both iodomethane and methane, but could also be due to a methyl radical. It is observed that even at the lowest CH_3I exposures, methane desorption is apparent. The insert of Fig. 4(c) compares the 15 and 16 amu desorption profiles at a CH_3I exposure of 1 L. The mass spectrometer ionizer fragmentation ratio for 15 and 16 amu for methane is ~ 0.9 . This suggests that the desorption state at ~ 220 K contains a contribution from desorbing methyl radicals. Note that this state is not due to molecular iodomethane desorption since essentially no molecular desorption is found at an exposure of 1 L (Fig. 3(a)).

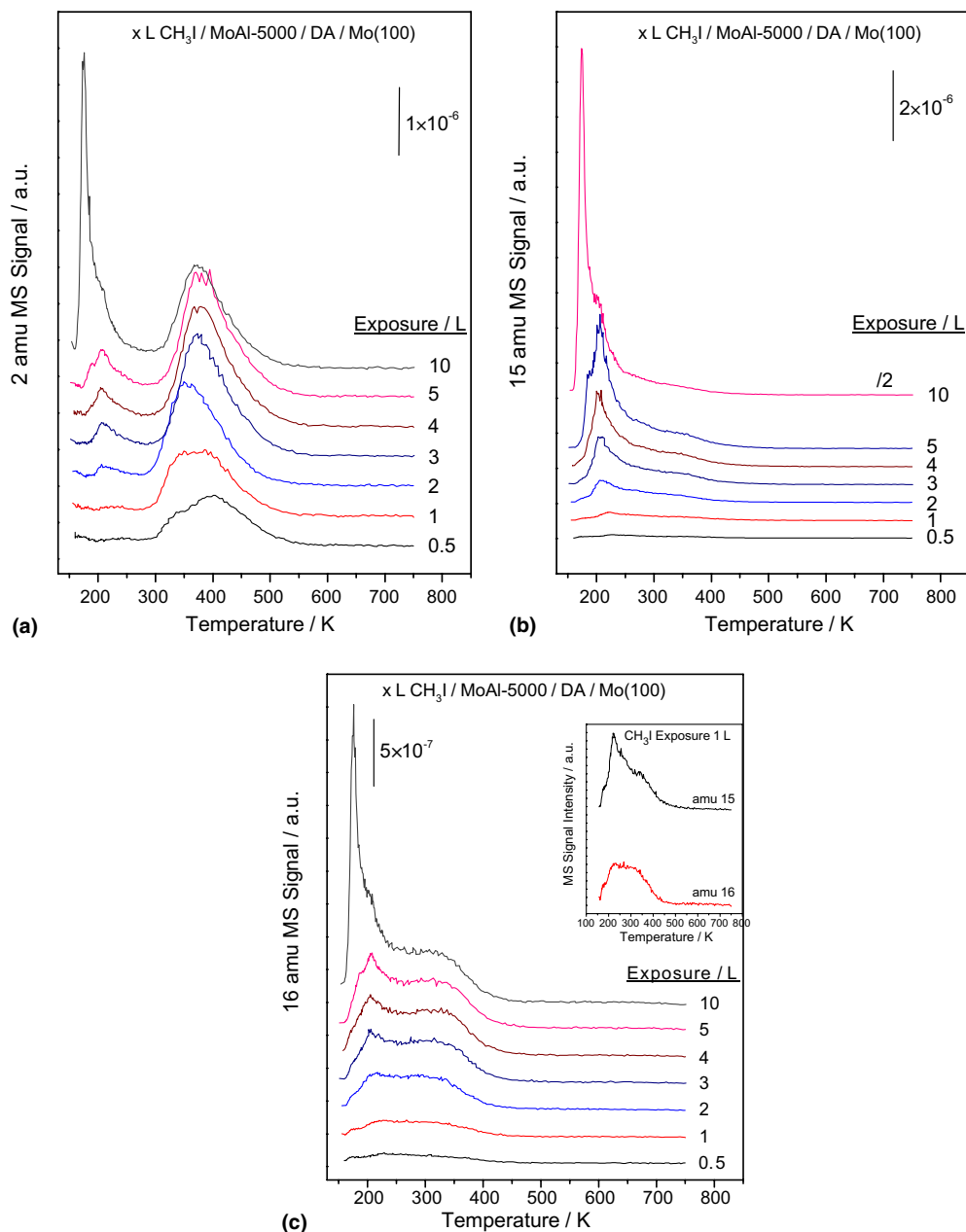


Fig. 4. (a) 2 (H_2), (b) 15 (CH_3), and (c) 16 (CH_4) amu temperature-programmed desorption spectra of iodomethane adsorbed on a MoAl film at 150 K collected using a heating rate of 10 K/s, as a function of CH_3I exposure. Iodomethane exposures are marked adjacent to the corresponding spectrum. The 15- and 16-amu spectra for a 1 L iodomethane exposure are compared to the inset in (c).

The formation of higher-molecular-weight products is explored in the spectra shown in Fig. 5. The data in Fig. 5(a) (at a CH_3I exposure of 5 L) show intense 26 and 27 amu signals at

~ 210 K indicating ethylene formation. The origin of the sharp feature at 27 amu below 200 K is not very clear. Since this commences at the same temperature as multilayer CH_3I desorption, it is

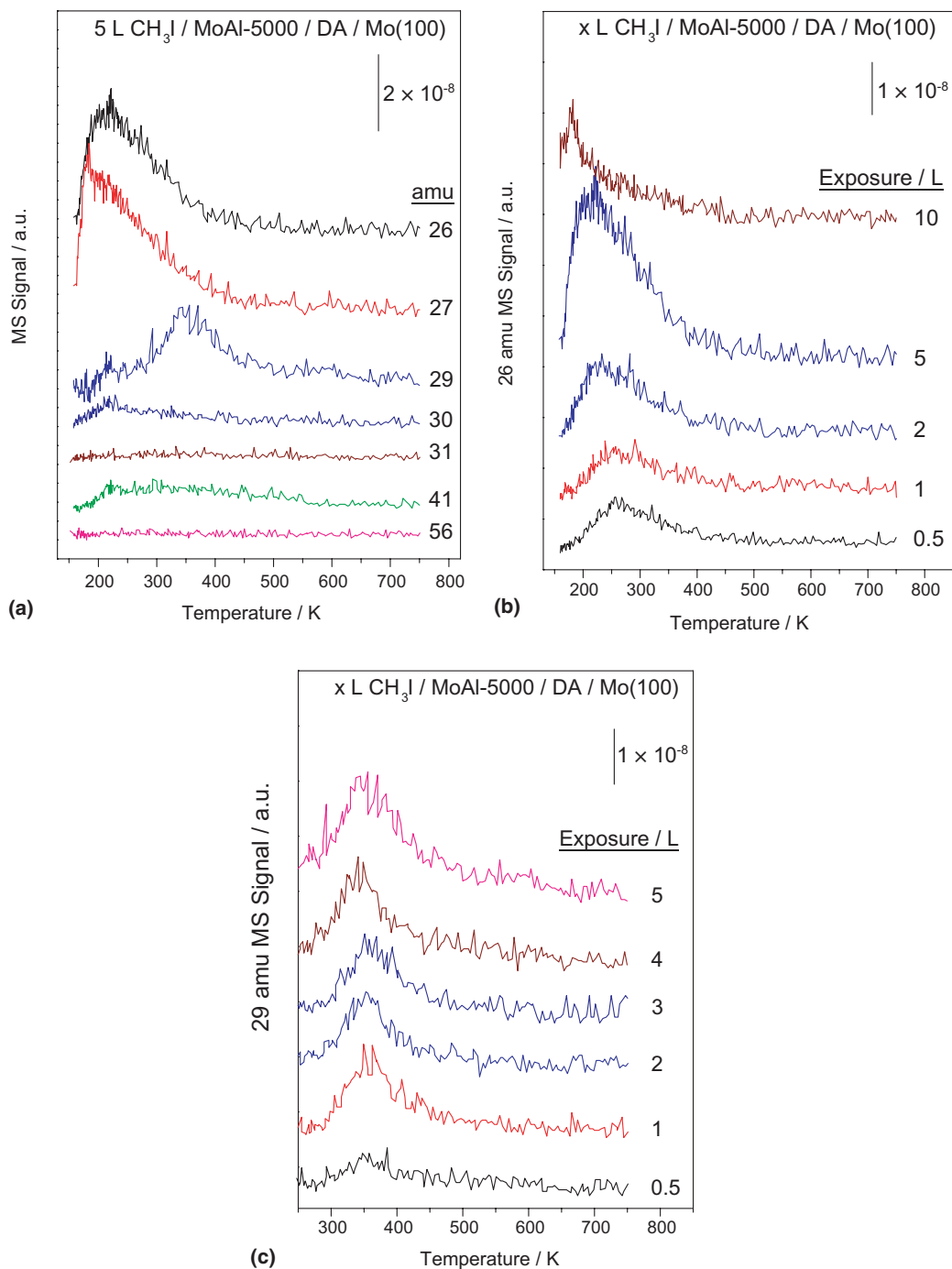


Fig. 5. (b) 26 (C_2H_2) and (c) 29 amu temperature-programmed desorption spectra of iodomethane adsorbed on a MoAl film at 150 K collected using a heating rate of 10 K/s, as a function of CH_3I exposure. Iodomethane exposures are marked adjacent to the corresponding spectrum. Fig. 5(a) display the spectra collected at various masses following 5 L iodomethane exposure, where the monitored masses are marked adjacent to the corresponding spectrum.

therefore assigned to species formed within the mass spectrometer ionizer. A small 30-amu signal is noted at ~ 210 K suggesting some ethane formation. Some propylene (41 amu) also desorbs over a rather wide temperature range but no C_4 species (at 56 amu) are detected. No methanol desorption (at 31 amu) is found. Fig. 5(b) displays the desorption profiles of ethylene (26 amu) as a function of exposure. The peak maximum decreases from ~ 250 K to ~ 210 K, and the desorption peak area increases, with increasing CH_3I exposure from 0.5 to 5 L, while almost no ethylene desorption is found at a CH_3I exposure of 10 L.

A 29 amu feature is found at ~ 350 K (Fig. 5(c)), which grows with increasing iodomethane exposure. Lack of desorption intensity at 30 or 31 amu at the same temperature allows the exclusion of ethane and oxygenates such as HCHO or CH_3OH as the origin for this state. Neither is this species due to C_2H_5I since this yields a rather intense amu 27 signal (verified by introducing C_2H_5I into the chamber and measuring its frag-

mentation pattern), so that this feature is ascribed to ethyl radical desorption.

The fate of the carbon and iodine adsorbed onto the surface after product desorption (Figs. 3–5) is explored in Fig. 6 by carrying out TPD experiments at a heating rate of 15 K/s following iodomethane adsorption and after annealing to ~ 750 K, where Fig. 6(a) presents the 28 amu (CO) desorption profiles and Fig. 6(b) the 63 amu (I^{2+}) spectra. CO desorbs at ~ 1200 K and it has been demonstrated previously that this is due to a reaction between deposited carbon and the alumina substrate [17,18]. The desorption peak area is plotted as a function of CH_3I exposure as an inset of Fig. 6(a). The desorption yield increases almost linearly from 0.5 to 4 L, reaches a maximum at 4 L, and then decreases at an exposure of 10 L. Fig. 6(b) shows that iodine desorbs between 800 and 1150 K and the integrated desorption peak area versus iodomethane exposure is plotted as an inset showing that the iodine coverage increases up to an exposure of 5 L and then saturates.

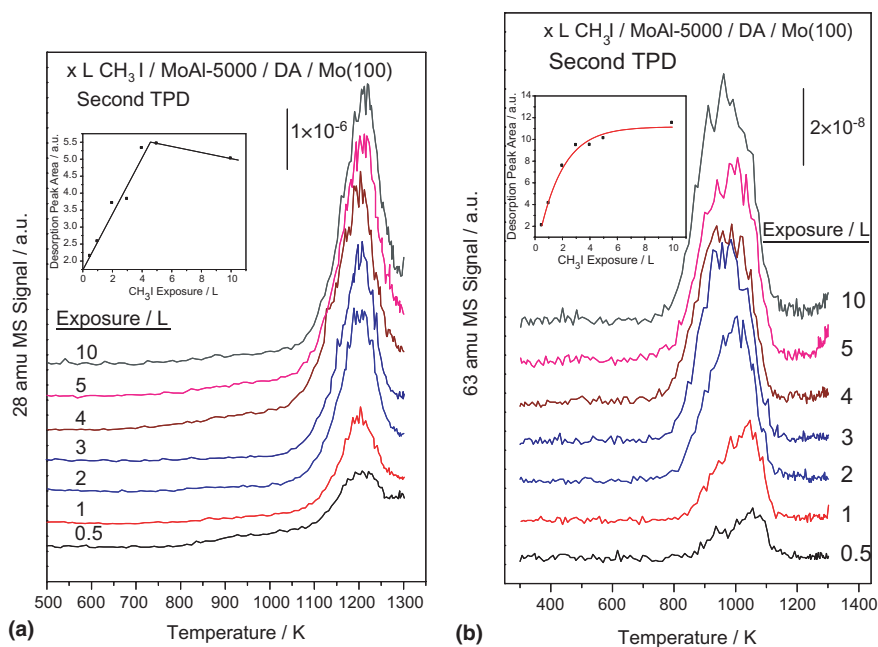


Fig. 6. (a) 28 (CO) and (b) 63 (I^{2+}) amu temperature-programmed desorption spectra of iodomethane adsorbed on a MoAl film at 150 K and then annealed to 750 K, collected using a heating rate of 15 K/s, as a function of CH_3I exposure. Iodomethane exposures are marked adjacent to the corresponding spectrum. Shown as insets in both spectra are the integrated desorption yields as a function of iodomethane exposure.

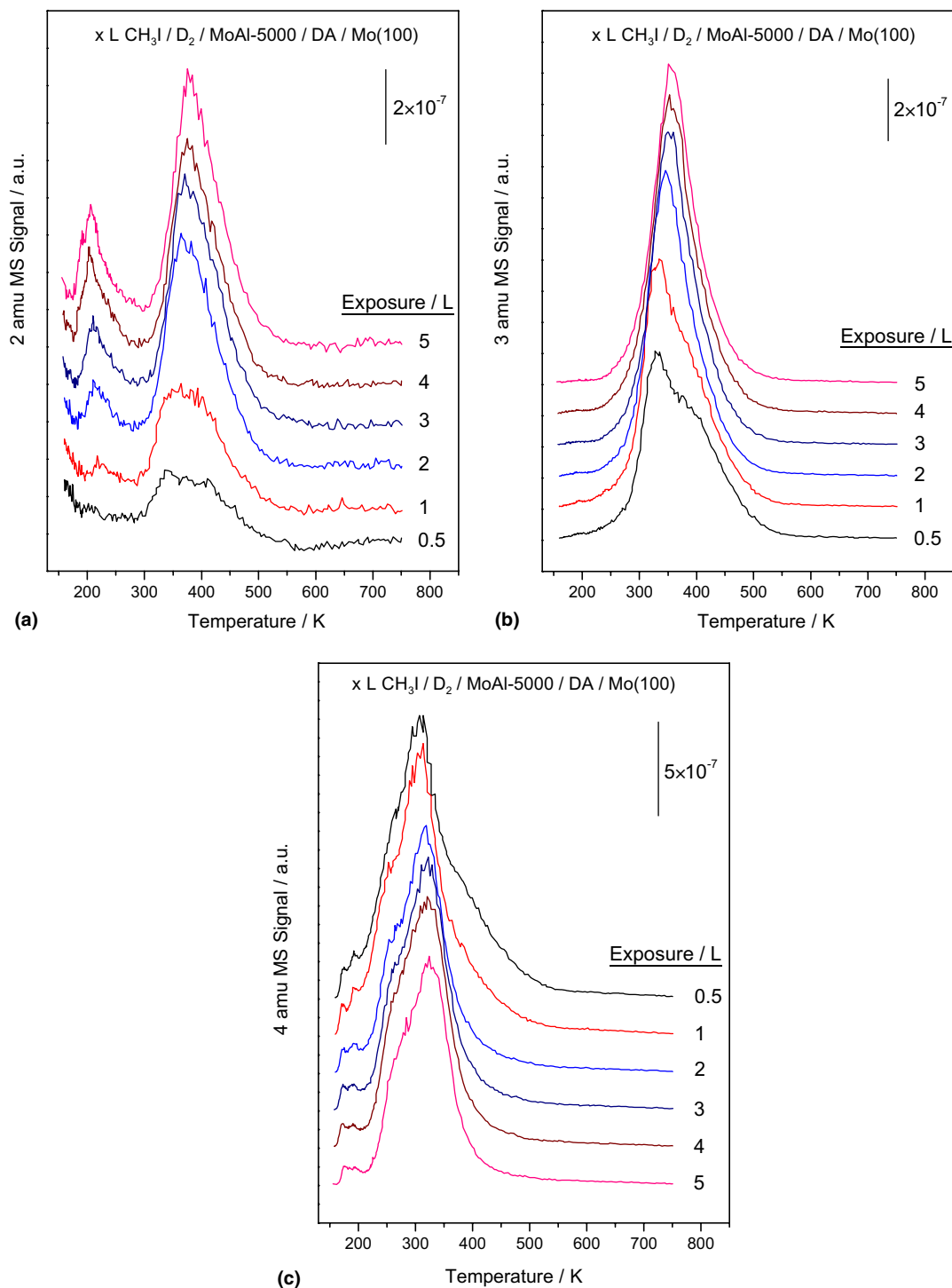


Fig. 7. (a) 2 (H_2), (b) 3 (HD) and (c) 4 (D_2) amu temperature-programmed desorption spectra of iodomethane adsorbed on a deuterium-saturated MoAl film at 150 K collected using a heating rate of 10 K/s, as a function of CH_3I exposure.

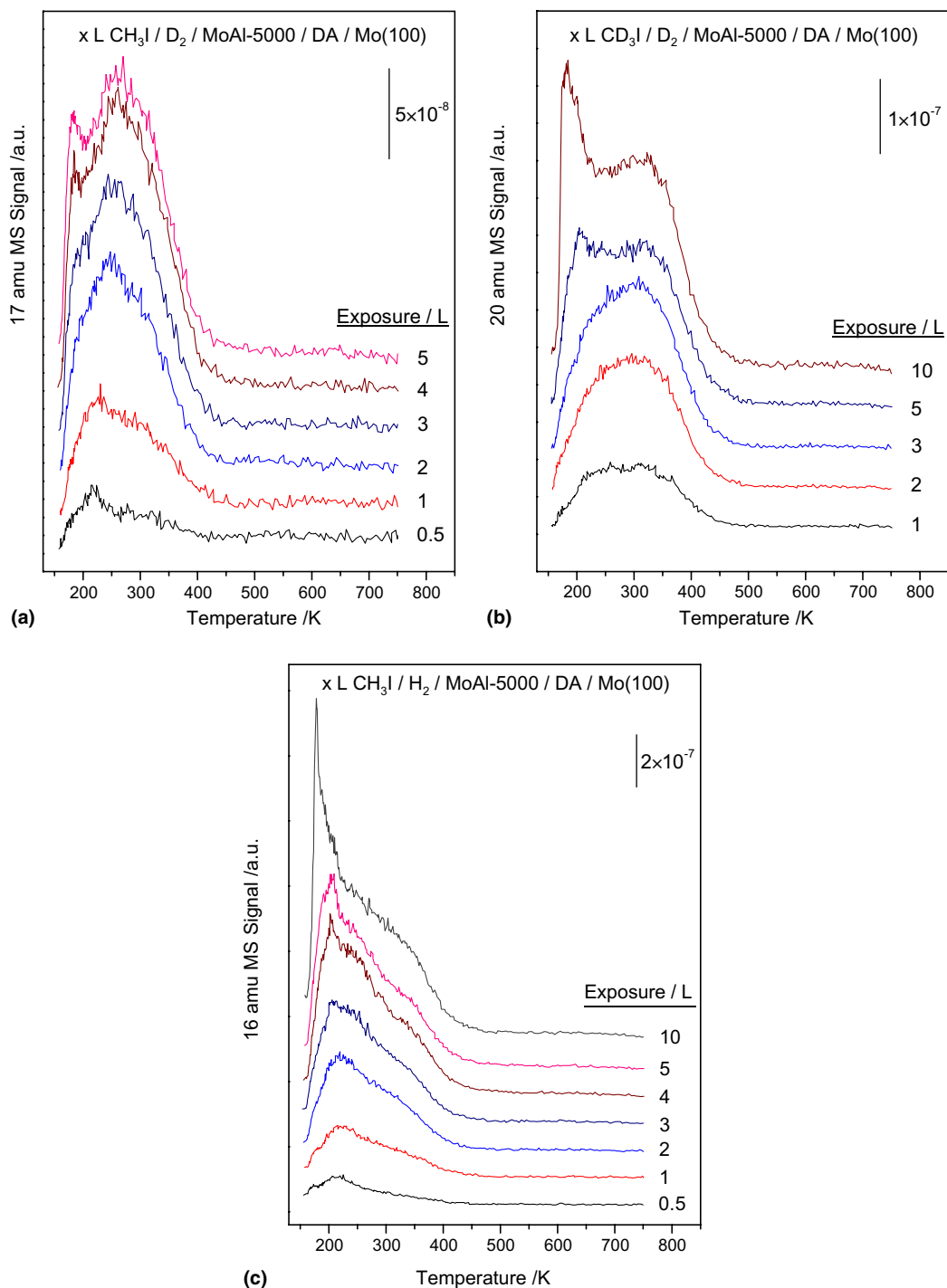


Fig. 8. (a) 17 (CH_3D) amu signal following CH_3I adsorption on a deuterium-saturated surface, (b) 20 (CD_4) amu signal, and (c) 16 (CH_4) amu signal following adsorption on a MoAl film collected using a heating rate of 10 K/s, as a function of iodomethane exposure where exposures are marked adjacent to the corresponding spectrum.

Fig. 7 displays desorption profiles of H_2 (Fig. 7(a)), HD (Fig. 7(b)) and D_2 (Fig. 7(c)) for various exposures of iodomethane to a deuterium-saturated (>20 L) MoAl film. These results show that background H_2 adsorption is reduced, indicated by the reduced signal intensity of the H_2 desorption state at ~ 410 K compared with that shown in Fig. 4(a). Note that the signal at ~ 210 K is due to fragmentation of CH_3I in the mass spectrometer ionizer. Lack of such a low-temperature signal at 3 amu indicates that there is no H-D exchange between CH_3I and D atoms. With increasing CH_3I adsorption, the D_2 desorption peak area decreases and the temperature range narrows. The surface D atoms are consumed by HD formation displayed in Fig. 7(b) and, as will be shown below, also by methyl hydrogenation.

Fig. 8(a) displays the corresponding amu 17 (CH_3D) desorption profiles as a function of CH_3I exposure. For comparison, the 16-amu (CH_4) profiles from $CH_3I + H_2$ and the 20-amu (CD_4) spectra from $CD_3I + D_2$ are also displayed in Fig. 8(b) and (c) respectively. Features in Fig. 8(b) at ~ 220 K, and the sharp, low-temperature peak at high iodomethane exposures, are likely to be due to species formed inside the mass spectrometer ionizer, and the spectra collected using deuterium (Fig. 8(a) and (c)) allow the methane desorption state to be more easily identified, where methane forms at both ~ 220 and 320 K. The low-temperature state is more pronounced than the high-temperature state. The desorption temperature of CD_4 is slightly higher than that of CH_4 and CH_3D , presumably due to a kinetic isotope effect [31].

4. Discussion

The surface chemistry of CH_3I on transition metal surfaces is, in many cases, rather complicated [21]. The first step, which is generally accepted to be C–I bond cleavage, occurs easily due to the relatively small C–I bond strength. The fate of the resulting methyl species, however, depends greatly on the nature of the surface and coverage. For surfaces that are inactive for dehydrogenation, for example, silver, methyl groups

couple at ~ 250 K to generate ethane [33]. For surfaces that weakly dissociate a small portion of the methyl groups, while the majority of these are thermal stable to high temperatures, for example, copper [34], surface hydrogen and methylene formation are the rate-determining steps. These are quickly consumed by intact methyl groups to form methane, ethylene and ethane at rather high temperatures (400 K). Surfaces that readily dissociate methyl species can be separated into two categories. Metals such as tungsten [35] completely dissociate methyl groups resulting in carbon deposition and only hydrogen is found to desorb. Metals like Ni [31,36,37], Pt [38], Pd [39] and Mo [23,24] dissociate a portion of methyl groups, while the rest remains intact at low temperatures. In these cases, methane and H_2 are the major gaseous products, and the methane evolution temperature is substantially lower than for copper. Methylene species are detected in these systems. However, these easily undergo further hydrogenation or decomposition so that carbon insertion reactions are either very minor or nonexistent. Consequently, higher hydrocarbons, even if they are formed, comprise a very small proportion of the gaseous products [20,21,31]. If these metals are modified, for example by oxygen, the reactive properties become closer to copper in terms of methyl dissociation so that higher hydrocarbons are more readily formed [40,41].

The chemistry of adsorbed methyl species on the MoAl alloy is richer than on either the individual molybdenum or aluminum surfaces. The only gaseous products formed following iodomethane on molybdenum single crystals [23,24] are methane and H_2 . Carbon and iodine deposition are found due to complete thermal decomposition and no higher hydrocarbons are detected. Methyl and methylidyne species are formed on aluminum, but no methylene species are found [25,26] and a small amount of carbon and iodine deposition is detected using Auger spectroscopy and scanning tunneling microscopy (STM).

Iodomethane dissociates relatively rapidly on the MoAl alloy film, where a portion dissociates even at 150 K, and dissociation is complete on heating to 250 K (Fig. 2(c)) with the remainder desorbing molecularly below 220 K (Fig. 3). Re-

removal of iodine from iodomethane is accompanied by the formation of metal-iodine bonds. While iodine could adsorb on molybdenum [23], iodine appears to bond preferentially to Al. Auger data (Fig. 1) provide direct evidence for this since the Al^0 signal intensity decreases following CH_3I adsorption.

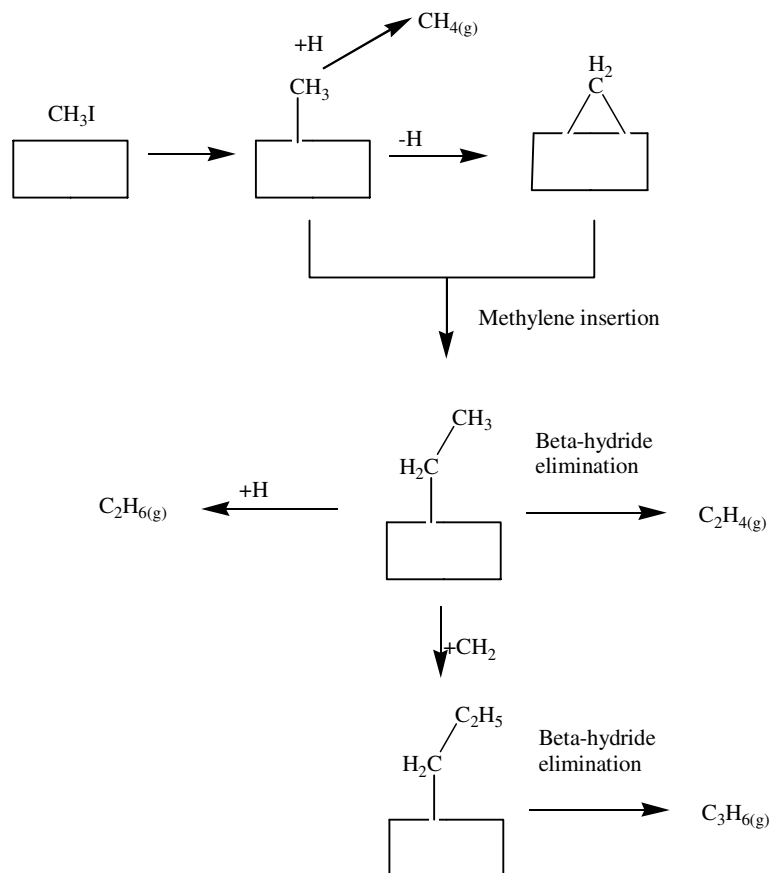
It is found that, at low CH_3I exposures, two iodine desorption states are evident at ~ 220 and ~ 400 K (inset, Fig. 3(b)). The first state has the same desorption temperature as CH_3I adsorbed on the alloy and is therefore assigned to cracking of molecular CH_3I in the mass spectrometer ionizer. Note, however, that no molecular desorption is found at CH_3I exposures below 2 L (Fig. 2(a)) and this may be due to the lower sensitivity of the mass spectrometer at higher masses. The ~ 400 K state, however, is due to iodine containing species other than CH_3I . Fig. 2(d) reveals that the iodine coverage decreases slightly between 250 and 800 K, consistent with the TPD results (Fig. 3(b)). Hare et al. [42] have studied the thermal chemistry of CH_2I_2 on $\text{Al}(111)$ and found that AlI_3 desorbs from the surface between 380 and 420 K, and iodine-containing organoaluminum compounds desorb at even higher temperatures. This state is therefore tentatively ascribed to AlI_3 desorption or evolution of iodine containing organoaluminum compounds. Note, however, this assignment is not unambiguous since the reactivity of aluminum within the alloy may be drastically different from pure aluminum.

Heating the surface up to ~ 400 K causes several surface reactions of the adsorbed methyl species including radical ejection, hydrogenation, oligomerization and dehydrogenation, the latter reaction giving rise to carbon deposition onto the surface (Figs. 1 and 2(b)). Carbon is removed as CO at ~ 1200 K due to reaction between deposited carbon and the alumina substrate [14,18].

Adsorbed methyl groups self-hydrogenate to yield methane between ~ 200 and 350 K (Fig. 4(c)), while presaturating the surface with hydrogen substantially increases the methane yield (Fig. 8), and the peak temperature increases with increasing iodomethane exposures and therefore methyl coverage. This implies that the hydrogenation activation energy increases with coverage. It

would be anticipated that a second-order reaction such as methyl plus hydrogen recombination should decrease in desorption temperature with increasing methyl coverage [43]. A change in methyl adsorption geometry has been found on $\text{Pd}(111)$ as a function of methyl coverage [39] and this effect may be due to methyl groups that are tilted at low coverages being easier to hydrogenate than more perpendicular methyl species that may form at higher coverages.

The data of Fig. 5 show that higher hydrocarbons are formed on the alloy surface. Ethylene desorption is detected at ~ 240 to 260 K depending on initial methyl coverage (Fig. 5(b)). A small amount of ethane evolves at approximately the same temperature. Two reaction pathways may account for ethylene formation. First, ethylene could be formed by an initial methyl dehydrogenation reaction to yield methylene species that insert into the C–Mo bond of the methyl group forming an adsorbed ethyl species. Such a reaction pathway, relevant to chain propagation in Fischer–Tropsch synthesis, has been proposed previously [20,21]. The resulting ethyl species can hydrogenate to yield ethane (30 amu, Fig. 5(c)), or undergo β -hydride elimination to produce ethylene (Fig. 5(a)). Second, ethylene could form by coupling of methylene species without involving an ethyl intermediate. The similar desorption temperature of ethylene and ethane, however, suggests that a common intermediate is involved. Ethyl radicals are also found to desorb at ~ 350 K (Fig. 5(b)) suggesting that an ethyl group is a common intermediate. Note that ethane could also originate from a direct coupling of methyl groups. This is not likely though, because of the similarity between the kinetics of ethylene and ethane formation, and the higher ethylene yield [31]. In addition to these reactions, a small portion of ethyl species can undergo further methylene insertion to yield propylene, while the chain propagation probability is not sufficiently large for any C_4 products to be detected. It is worth pointing out that ethylene formation is found within a narrow temperature (~ 250 K), while methane production proceeds within a wide temperature range up to ~ 350 K. This indicates that, within the temperature range where these species are formed, methyl species



dominate on the surface. Methylene species can be formed at rather low temperatures, while this undergoes rapid insertion followed by β -hydride elimination or hydrogenation reactions to form higher hydrocarbons. The proposed higher hydrocarbon formation pathways are summarized in Scheme 1.

The unique reactivity of the MoAl for higher hydrocarbon formation may be due to two effects, either electronic or geometric. In the first effect, molybdenum can gain electrons by alloying with aluminum, causing a larger d-band occupancy, to become electronically more like a noble metal. It is well known that transition metals with filled d bands such as copper efficiently catalyze carbon insertion reactions. Second, it could also be due to the blocking of reactive sites on the surface by

co-ordination to aluminum and the resulting iodine, which inhibits the complete dehydrogenation of the resulting surface methyl species allowing intermediate methylene species to be stabilized for a sufficient time to allow insertion into the methyl-surface bond. It should be mentioned that iodine adsorption does have some effect on the final product distribution. While this does not affect ethyl group formation (Fig. 5(c)), β -hydride elimination is diminished at the highest CH_3I exposures (Fig. 5(b)).

5. Conclusions

Iodomethane adsorbs both dissociatively and molecularly at 150 K on a MoAl alloy film formed

by reacting $\text{Mo}(\text{CO})_6$ with dehydroxylated alumina at 700 K and heating to 1500 K. Dissociation into methyl species and adsorbed iodide is complete by ~ 200 K, and is accompanied by desorption of molecular iodomethane. The iodine appears to adsorb preferentially on aluminum. The resulting adsorbed methyl species can either thermally decompose to yield hydrogen and adsorbed carbon, desorb as methyl radicals, or hydrogenate to methane. Oligomerization to ethylene and propylene is found as well as the formation of a small amount of ethane. This reaction appears to proceed via the insertion of a methylene species into the methyl-surface bond to form an adsorbed ethyl species, which can either desorb directly as a radical, form ethylene by β -hydride elimination, or hydrogenate to ethane. Additional insertion of a methylene species into the ethyl-surface bond forms a propyl species, which also reacts by β -hydride elimination to yield propylene. No higher oligomers are detected.

Acknowledgement

We gratefully acknowledge support of this work by the Chemistry Division of the National Science Foundation under grant no. CTS-0105329.

References

- [1] A. Brenner, *J. Mol. Catal.* 5 (1979) 157.
- [2] E. Davie, D.A. Whan, C. Kemball, *J. Catal.* 24 (1972) 272.
- [3] J. Smith, R.F. Howe, D.A. Whan, *J. Catal.* 34 (1974) 191.
- [4] R. Thomas, J.A. Moulijn, *J. Mol. Catal.* 15 (1982) 157.
- [5] A. Brenner, R.L. Burwell Jr., *J. Am. Chem. Soc.* 97 (1975) 2565.
- [6] A. Brenner, R.L. Burwell Jr., *J. Catal.* 52 (1978) 353.
- [7] R.F. Howe, *Inorg. Chem.* 15 (1976) 486.
- [8] A. Kazusaka, R.F. Howe, *J. Mol. Catal.* 9 (1980) 183.
- [9] K.P. Reddy, T.L. Brown, *J. Am. Chem. Soc.* 117 (1995) 2845.
- [10] A. Zecchina, E.E. Platero, C.O. Areán, *Inorg. Chem.* 27 (1988) 102.
- [11] R.F. Howe, I.R. Leith, *J. Chem. Soc., Faraday Trans. I* 69 (1973) 1967.
- [12] W.M. Shirley, B.R. McGarvey, B. Maiti, A. Brenner, A. Cichowlas, *J. Mol. Catal.* 29 (1985) 259.
- [13] M. Kaltchev, W.T. Tysoe, *J. Catal.* 193 (2000) 29.
- [14] M. Kaltchev, W.T. Tysoe, *J. Catal.* 196 (2000) 40.
- [15] Y. Wang, F. Gao, M. Kaltchev, D. Stacchiola, W.T. Tysoe, *Catal. Lett* 91 (2003) 88.
- [16] Y. Wang, F. Gao, M. Kaltchev, W.T. Tysoe, *J. Mol. Catal. A: Chemical* 209 (2004) 135.
- [17] Y. Wang, F. Gao, W.T. Tysoe, *J. Mol. Catal. A: Chem.* 236 (2005) 18.
- [18] Y. Wang, F. Gao, W.T. Tysoe, *J. Mol. Catal. A: Chem.* 235 (2005) 173.
- [19] H.H. Hwu, M.B. Zellner, J.G. Chen, *J. Catal.* 229 (2005) 35.
- [20] F. Zaera, *Chem. Rev.* 95 (1995) 2651.
- [21] B.E. Bent, *Chem. Rev.* 96 (1996) 1361.
- [22] Y. Wang, F. Gao, W.T. Tysoe, in preparation.
- [23] G. Wu, H. Molerio, W.T. Tysoe, *Surf. Sci.* 397 (1998) 179.
- [24] G. Wu, M. Kaltchev, W.T. Tysoe, *Surf. Rev. Lett.* 6 (1999) 13.
- [25] J.G. Chen, T.P. Beebe Jr., J.E. Crowell, J.T. Yates Jr., *J. Am. Chem. Soc.* 109 (1987) 1726.
- [26] S. Mezheny, D.C. Sorescu, P. Maksymovych, J.T. Yates Jr., *J. Am. Chem. Soc.* 124 (2002) 14202.
- [27] W.J. Wytenburg, R.M. Lambert, *J. Vac. Sci. Technol. A* 10 (1992) 3597.
- [28] D. Briggs, M.P. Seah, *Practical Surface Analysis: Auger and X-Ray Photoelectron Spectroscopy*, John Wiley & Sons, 2004.
- [29] B.R. Strohmeier, *Surf. Sci. Spectra* 3 (1995) 135.
- [30] F. Zaera, H. Hoffmann, *J. Phys. Chem.* 95 (1991) 6297.
- [31] H. Guo, F. Zaera, *J. Phys. Chem. B* 108 (2004) 16220.
- [32] S. Chaturvedi, D.R. Strongin, *Langmuir* 13 (1997) 3162.
- [33] X.-L. Zhou, J.M. White, *Surf. Sci.* 241 (1991) 270.
- [34] C.-M. Chiang, T.H. Wentzlaff, B.E. Bent, *J. Phys. Chem.* 96 (1992) 1836.
- [35] X.-L. Zhou, C. Yoon, J.M. White, *Surf. Sci.* 206 (1988) 379.
- [36] S. Tjandra, F. Zaera, *J. Catal.* 144 (1993) 361.
- [37] S. Tjandra, F. Zaera, *J. Catal.* 147 (1994) 598.
- [38] F. Zaera, *Langmuir* 7 (1991) 1998.
- [39] D. Stacchiola, Y. Wang, W.T. Tysoe, *Surf. Sci.* 524 (2003) 173.
- [40] S.H. Kim, P.C. Stair, *J. Phys. Chem. B* 104 (2000) 3035.
- [41] K.A. Dickens, P.C. Stair, *Langmuir* 14 (1998) 1444.
- [42] M. Hara, K. Domem, M. Kato, T. Onishi, H. Nozoye, *J. Phys. Chem.* 96 (1992) 2637.
- [43] P.A. Redhead, *Vacuum* 12 (1962) 203.